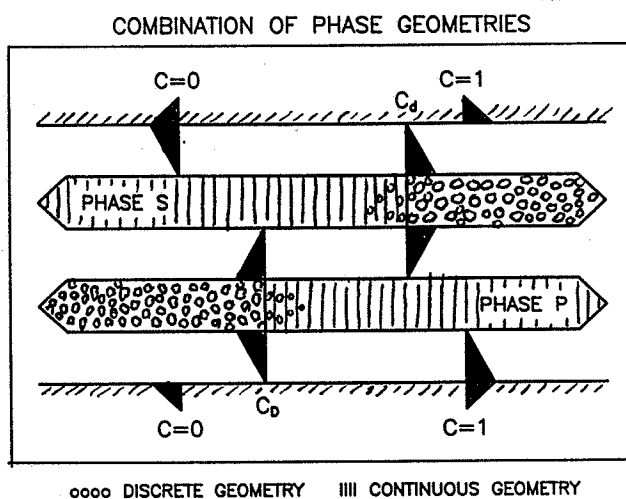# SHRINKAGE, SWELLING, AND STIFFNESS OF COMPOSITES
strain and stress caused by hygro-thermal action and solidification or freezing of liquid impregnant

Lauge Fuglsang Nielsen

COMBINATION OF PHASE GEOMETRIES

oooo DISCRETE GEOMETRY   IIII CONTINUOUS GEOMETRY

Building Materials Laboratory
Technical University of Denmark
Building 118
DK-2800 Lyngby, Denmark

SHRINKAGE, SWELLING, AND STIFFNESS OF COMPOSITES
strain and stress caused by hygro-thermal action and solidification or freezing of liquid impregnant

Lauge Fuglsang Nielsen

Physics and Materials Division
Engineering Academy
Technical University of Denmark
DK-2800 Lyngby, Denmark

Abstract: A theory has previously been developed by the author which predicts stiffness and internal stresses of two-phase materials with arbitrary phase geometry. The theory has been successfully applied in research on stiffness and strength of porous materials and damping of impregnated materials. In this article the theory forms the basis of a rational method subsequently developed to predict shrinkage, swelling, and internal stresses of composite materials where the constituent phases experience hygro-thermal strain or volume change by solidification of liquid impregnant (including ice formation in porous materials). The method applies for any phase geometry. Three special composites, however, are considered in more details: Particle reinforced materials (like concrete and chopped fiber composites), Powder composites (compacted powders), and Lamella composites (where any phase has a continuous geometry like many impregnated porous materials). Examples are given. Among others: Thermal expansion of salt infected tile, Expansion and damage of porous materials due to ice formation in pores. An algorithm is presented by which the numerical calculations involved are easily made on a small computer. Some possibilities of damage detection are briefly discussed.

As a curiosum it is shown how the stiffness results of the method developed can easily be used also to predict a number of other physical properties of composites with arbitrary internal geometry. Examples are thermal and electric conductivity, dielectric constant and magnetic permeability.

Keywords: Composite material, Porous material, Phase geometry, Hygro-thermal strain, Shrinkage, Swelling, Internal stress, Stiffness, Impregnation, Frost damage, Damage detection, Thermal conductivity, Electrical conductivity, Dielectric constant.

I. INTRODUCTION

A rational prediction method is developed for *shrinkage, swelling,* and *internal stresses* in *isotropic composite materials* of *arbitrary phase geometry*. The composites are two-phase materials exposed to *hygro-thermal action* (volumetric deformation caused by change of moisture and temperature) or volume change by *solidification* of liquid impregnant (*ice formation* included).

No prediction method considering such behavior of composite materials can be better than the method applied to predict the bulk modulus of the material considered. This is a consequence of results obtained in the paper that stress and strain in a composite subjected to hygro-thermal action can be determined exactly when composite bulk modulus is known. Thus, from a users point of view the most important feature of a rational prediction method is its ability to handle geometrical information defining the composites considered – whether they are fiber composites, for example, or impregnated porous materials.

This point is considered in Section II as the first step of a rational "hygro-thermal" prediction method: Appropriate parts of the authors own composite stiffness theory (1) are summarized, adapted, and justified to form a proper basis of prediction. Incidentally, the stiffness

theory referred to has recently been used successfully by the author (e.g. 2,3,4) in studies on strength-stiffness relations of porous materials and elasticity and damping of impregnated materials where the question of phase geometry is also of vital interest.

The final steps in developing a hygro-thermal prediction method are taken in Sections III and IV where composite stiffness information and information on hygro-thermal and other volumetric actions are brought together in an analysis producing the prediction results wanted. An algorithm is hereby given where input data and steps of calculations are arranged in a way appropriate for computer prediction.

Applications of the prediction method are demonstrated in Section V considering thermal expansion of salt infected tile, for example, and expansion and damage of bricks due to ice formation in pores. As previously indicated, the method applies in general for any phase geometry. Three special composites, however, are considered in more details: Particle reinforced materials (like concrete and chopped fiber composites), Powder composites (compacted powders), and Lamella composites (where any phase has a continuous geometry like many impregnated porous materials).

Curiosum: The stiffness results presented in the paper can be used easily also to predict a number of other physical properties of composites of arbitrary internal geometry. Examples are thermal and electric conductivity, dielectric constant and magnetic permeability. This feature is considered in Appendix A and referred to in Section VI where possibilities of damage detection in composite materials are briefly discussed.

The terminology used in the stress-strain analysis considering hygro-thermal action is shown in the following list.

Volume and Stiffness

V_i	Volume of phase $i = S,P$
$c = V_P/(V_S + V_P)$	Volume concentration of phase P
$1 - c$	Volume concentration of phase S
E_i	Young's modulus of phase $i = S,P$
v_i	Poisson's ratio of phase $i = S,P$
$K_i = E_i/(1-2v_i)/3$	Bulk modulus of phase $i = S,P$
$G_i = E_i/(1+v_i)/2$	Shear modulus of phase $i = S,P$
$n = E_P/E_S$	Young stiffness ratio
$n_K = K_P/K_S$	Bulk stiffness ratio
$n_G = G_P/G_S$	Shear stiffness ratio
K^*	Bulk modulus of composite material
$k^* = K^*/K_S$	Relative bulk modulus of composite material

Stress and strain

σ_{kk}	Volumetric stress on composite material
$\epsilon_{kk} = \sigma_{kk}/3K^*$	Volumetric strain of composite material
$\sigma_{i,kk}$	Volumetric stress of phase $i = S,P$
$\epsilon_{i,kk} = \sigma_{i,kk}/K_i$	Volumetric strain of phase $i = S,P$
$\alpha_{i,kk}$	Free vol. hygro-thermal strain, phase $i = S,P$
α_{kk}	Free vol. hygro-thermal strain of composite

Bulk stiffness ratio, n_K, and shear stiffness ratio, n_G, are related to Young stiffness ratio, n, and associated Poisson's ratios as follows

$$n_K = n \frac{1 - 2v_S}{1 - 2v_P} \qquad n_G = n \frac{1 + v_S}{1 + v_P} \qquad \Theta_S = 2 \frac{1 - 2v_S}{1 + v_S} \qquad (1)$$

where Θ_S is an auxiliary parameter used in the subsequent section. It is noticed that

$$v_S = v_P = 0.2 \qquad \Rightarrow \qquad n_K = n_G = n \quad and \quad \Theta_S = 1 \qquad (2)$$

II. STIFFNESS OF COMPOSITE MATERIAL

It has previously been mentioned that bulk modulus prediction is the very important basic part of any prediction method considering the behavior of composites being subjected to hygro-thermal and other volumetric actions. In this section we obtain this basic information from (1) which considers stiffness in general of isotropically linear elastic two-phase materials with arbitrary phase geometry.

The information from (1) is adapted for the present purpose and summarized in a user-orientated form without any theoretical verifications. Some examples, however, are given which justify the applicability of the method. Comments are also given which relate the method presented to other stiffness prediction methods available in the literature.

The bulk modulus expressions given in this section apply in principle also when shear modulus and Young's modulus of composite materials are considered. Only a few simple modifications explained in (1) have to be introduced. Good estimates, however, can be obtained directly when $v_S = v_P = 0.2$.

Geometry

Critical concentrations: In general we consider two-phase materials where both phases may change their geometries from discrete to fully continuous at increasing respective concentrations. This feature is illustrated in Figure 1 where each phase is represented by a "geometry cylinder". The *critical concentrations* (of phase P) are c_d where the phase S geometry becomes discrete, and c_D where the phase P geometry leaves the state of being discrete. A critical concentration defines the "middle" of a transition area. At the "continuous side" there is a partly continuous zone with some discrete elements. At the "discrete side" there are discrete elements "getting ready" to conglomerate into elements of continuous geometries.

The two geometry cylinders can be shifted relative to each other defining different types of composites. The critical concentration c_d can be shifted from 0 to infinity defining discrete and continuous phase geometry respectively of phase S at any concentration. The critical concentration c_D can be shifted from 1 to negative infinity defining discrete and continuous phase geometry respectively of phase P at any concentration. Critical "concentrations" outside the area c = 0 - 1 do not have an immediate physical meaning. Still, however, they define the main trends of change in phase geometry

Special composites are classified according to their critical concentrations. Ideal *Particle reinforced materials* have $(c_d, c_D) = (\infty, 1)$ corresponding to discrete particles in a continuous matrix. Ideal *Powder composites* have $(c_d, c_D) \approx (0.5, 0.5)$ corresponding to a compacted mixture of phase P and phase S powders. Ideal *Lamella composites* have $(c_d, c_D) = (\infty, -\infty)$ defining both phases to have continuous geometries like ribbons or dendrites.
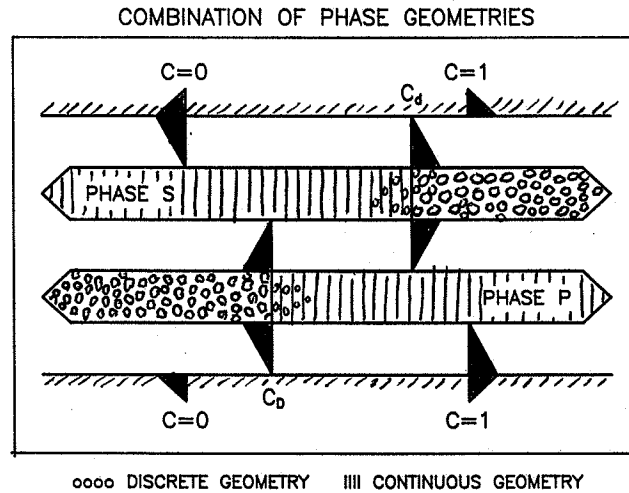

Figure 1.   Phase geometries and combinations of geometries considered in the paper.

Shape factors: These factors, μ_o and μ'_o, consider the low concentration geometrical complexity of phase P (at c = 0) and phase S (at c = 1) respectively. In general shape factors are smaller than 1 (spherical particles) and greater than 0 (spherical shells). An estimate of shape factors applying to arbitrary geometries in between these extremes are obtained from Table 1.

Predominant phase geometrytry at small respective volume concentrations	Shape factor μ_o, μ'_o	Example
Enveloping network tending to subdivide the other phase into particles	Low (0-0.4)	crumbled plate-work
Lamella, f. ex Dendrites, Ribbons	Medium (0.3-0.7)	impregnation
Particles defined by enveloping network of the other phase	High (0.6-1)	needles grains

Table 1.   Shape factors of composite materials as a function of phase geometry. Orders of magnitudes.

Bulk modulus

The bulk modulus of an isotropic two phase material can be predicted by the following expression

$$k^* = \frac{K^*}{K_S} = \frac{n_K + \langle\Theta\rangle[1 + c(n_K - 1)]}{n_K + \langle\Theta\rangle - c(n_K - 1)} \qquad (3)$$

where the influence of phase geometry is introduced by the *geometry function*, $\Theta_S \leq \langle\Theta\rangle \leq n_G\Theta_S$,

$$\frac{\langle\Theta\rangle}{\Theta_S} = 0.5[\mu + n_G\mu' + \sqrt{(\mu + n_G\mu')^2 + 4n_G(1 - \mu - \mu')}] \qquad (4)$$

The so-called *shape functions*, μ and μ', are defined as follows by the critical concentrations and shape factors previously explained,

$$\mu = \mu(c) \qquad\qquad\qquad monotonically\ decreasing$$
$$0 \leq \mu_o = \mu(0) \leq 1 \quad ; \quad \mu(c_d) = 0 \quad ; \quad c_d \geq 0 \qquad (5)$$

$$\mu' = \mu'(c) \qquad\qquad\qquad monotonically\ increasing$$
$$0 \leq \mu'_o = \mu'(1) \leq 1 \quad ; \quad \mu'(c_D) = 0 \quad ; \quad c_D \leq 1;\ c_D \leq c_d \qquad (6)$$

Interaction between phases and individual phase elements is proportional to the derivatives of the shape functions.

Composite	c_d	c_D	μ_o	μ'_o
H/S-bounds	∞	1	1	0
	0	$-\infty$	0	1
Budiansky	0.5	0.5	1	1
Particulate	> 1	1	0.8	0.8
powder	0-1	0-1	0.7	0.7
lamella				
and plates	>1	<0	<0.7	<0.7

Table 2. Geometrical parameters for composites. Examples.

The extreme phase geometries previously referred to are defined by by $(\mu,\mu') \equiv (1,0)$ and $(\mu,\mu') \equiv (0,1)$ corresponding to non-interacting phase P spheres in a continuous phase S matrix and non-interacting phase S spheres in a continuous phase P matrix respectively. The geometry functions associated are given by Equation 4. We get $\langle\Theta\rangle \equiv \Theta_S$ and $\langle\Theta\rangle \equiv n_G\Theta_S$ respectively by which the Hashin-Shtrikman's (H/S) bounds (5) are correctly described by Equation 3. The exact bulk modulus solution obtained by Hashin (6) for the so-called CSA-material is closely related to the H/S boundary expressions. In the present context the exact solution is described by Equation 3 with $\langle\Theta\rangle \equiv \Theta_S$. (CSA = Composite Spheres Assemblage = a tight mixture of congruent spherical composite elements each consisting of a matrix, centrally reinforced with a spherical particle of constant concentration).

Porous material: Phase P is an empty pore system. The porosity is c and stiffness is 0 involving $n_G = 0$. The bulk modulus of a porous material is obtained from Equation 3 as follows

$$k^*_o = \frac{K^*_o}{K_S} = \Theta_o \frac{1 - c}{\Theta_o + c} \qquad (7)$$

$$\Theta_o = \Theta_S\mu \qquad\qquad\qquad ; (\equiv 0\ at\ c > c_d) \qquad (8)$$

5

At low porosities we get the following linear approximation,

$$k^*_o \approx 1 - (1 + \frac{1}{\mu_o \theta_S})c \qquad ; \ (low \ porosity) \qquad (9)$$

Shape functions: The basic shape functions used in this paper are the following with $\mu(c > c_d) = -\mu(2c_d - c)$ and $\mu'(c < c_D) = -\mu'(2c_D - c)$,

$$\mu = \mu_o (\frac{c_d - c}{c_d})^M \qquad ; \qquad \mu' = \mu_o '(\frac{c - c_D}{1 - c_D})^M \qquad (10)$$

where the *interaction power* $M \geq 0$ modifies interaction relative to the "moderate" one described by $M = 1$. It has previously been indicated that interaction effects between phases and individual phase elements are proportional to the numerical slopes of μ and μ'. Thus, decreasing interaction is described by Equation 10 with increasing c_d, decreasing c_D, and/or decreasing M. (At $M = 0$ no interaction is present before it becomes "complete" at a critical concentration). It is concluded in (1) from FEM-analysis on bulk moduli of composites that $M = 1$ is appropriate when both critical concentrations are in the range, $c = 0 - 1$. Otherwise $M < 1$.

In the numerical evaluations of the present study we simplify matters by *introducing* $M \equiv 1$. This step is well justified when we at the same time modify the critical concentrations (outside $c = 0 - 1$) such that interaction (derivative of shape function) will not change significantly. An extreme example is that Equation 10 describes the same interaction and change of geometry in $c = 0 - 1$ with $(c_d, M) = (2, 0)$ and $(c_d, M) = (\infty, 1)$ respectively.
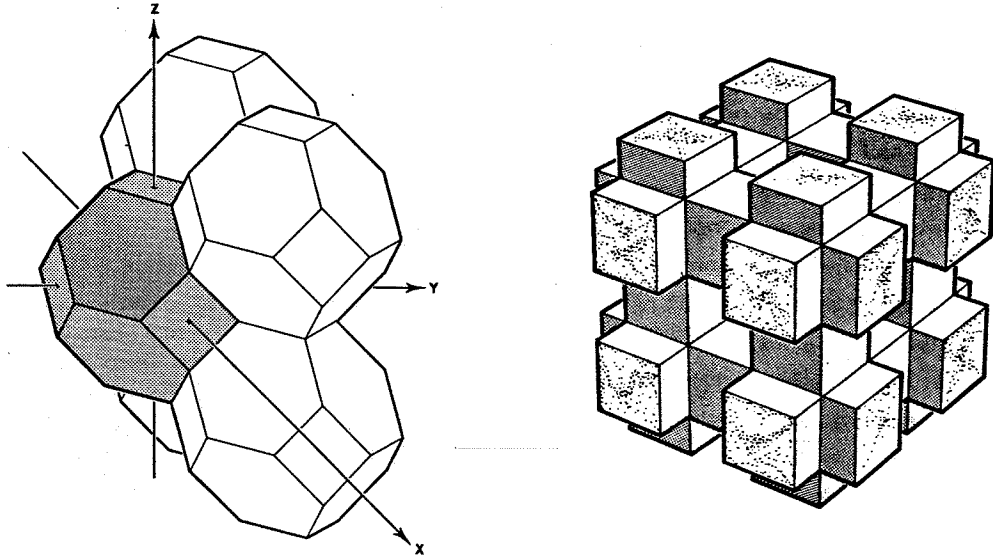

Figure 2. Basic elements of the TROC- and CR-materials. ■ The TROC-material is a perfect particle reinforced material. ■ The CR-material is a perfect (phase-symmetric) lamella material.

Some examples of composite descriptions are given in Table 2. Also shown in this table are geometrical parameters by which the H/S-

6

bounds previously referred to and the Budiansky SCS-solution (7) (Self Consistence Scheme) are predicted by the present theory.

Pseudo phase-symmetric composites: Pseudo phase-symmetric are composites where the geometry of phase P at concentration $c = c_P$ is identical to the phase S geometry at concentration (still of phase P), $c = 2c_{SYM} - c_P$, where the symmetry concentration, c_{SYM}, is given by

$$c_{SYM} = (c_d + c_D)/2 \qquad (11)$$

Given one shape function (master shape function), $\mu(c)$ or $\mu'(c)$, the other one is obtained as follows

$$\begin{aligned} \mu' &= \mu(c_d + c_D - c) \\ \mu &= \mu'(c_d + c_D - c) \end{aligned} \qquad (12)$$

The composite model considered by Budiansky (7) is one where phase P and phase S are spherical particles at $c = 0$ and $c = 1$ respectively. At any concentrations c and 1-c phase P and phase S respectively have identical geometries. In the present terminology the result obtained by Budiansky corresponds to $\mu = 1 - 2c$, meaning $c_{SYM} = c_d = c_D = 0.5$ *(real phase-symmetry)* together with $\mu_o = 1$ (and M = 1).

Many two-phase materials can be considered approximately as pseudo phase-symmetric composites. The master shape function must be chosen such that both shape factors, μ_o and $\mu'_o \leq 1$. This is safely obtained choosing μ from Equation 10 as master shape function when $c_{SYM} \geq 0.5$ and μ' when $c_{SYM} < 0.5$.

Curiosum: The following observation may be of interest exploring the possibilities of generalizing Equation 3 also to consider anisotropic composites by introducing "anisotropic" geometry functions: The Paul/Hansen's upper and lower bounds (8,9) are predicted by Equation 3 introducing $\langle \theta \rangle \rightarrow \infty$ and $\langle \theta \rangle \rightarrow 0$ respectively. Apparently $\langle \theta \rangle$ is in a way proportional to a "phase aspect ratio", A, defined by phase "length" parallel to "load" divided by phase "thickness" perpendicular to load. The materials models such defined by $A \approx \langle \theta \rangle = \infty$ and $A \approx \langle \theta \rangle = 0$ are exactly those used by Hansen (9) to establish the upper and lower bound respectively for stiffness of composites with unrestricted phase geometry.

Justification of prediction method

Finite element analysis (10,11) have been made to determine stiffness in general (bulk and shear) of the TROC-material and the CR-material illustrated in Figure 2. The TROC-material is a particle reinforced material consisting of identical composite elements each having the shape of a TRuncated OCtahedron. The composite element is reinforced by a centrally placed particle the shape and orientation of which are similar to the shape and orientation of the composite element itself. The CR-material is a CRoss reinforced pseudo phase-symmetric composite. Both models are cubically elastic. However, the results obtained by the FEM analysis are easily transformed to apply for isotropic mixtures.

The bulk modulus FEM-data shown by dots in Figure 3 are based on both phases having a Poisson ratio of 0.2. The theoretical results also shown are obtained by the method described in this section with

shape functions given by Equation 10. ▪ TROC-material: $(c_d, c_D, \mu_o, \mu'_o, -M) = (\infty, 1, 1, 0, 1)$. ▪ CR-material: $(c_d, c_D, \mu_o, \mu'_o, M) = (2, -1, 0.6, 0.6, 1)$.

An excellent agreement is observed between theory and (FEM)experiments. (This observation holds in (1) also when Poisson's ratios different from 0.2 and modified phase geometries are considered). It is further noticed from Figure 3 that the TROC-material has a bulk modulus very close to the exact result of the CSA-material previously referred to obtained by Hashin. The moduli of the CR-material are in general closest to the H/S-upper bounds. For the TROC-material this only applies when the stiffness ratio is less than unity.

It is now justified that the stiffness theory presented qualifies as a sound basis in the analysis made in the subsequent section on stress and strain in composite materials subjected to hygro-thermal and similar actions.
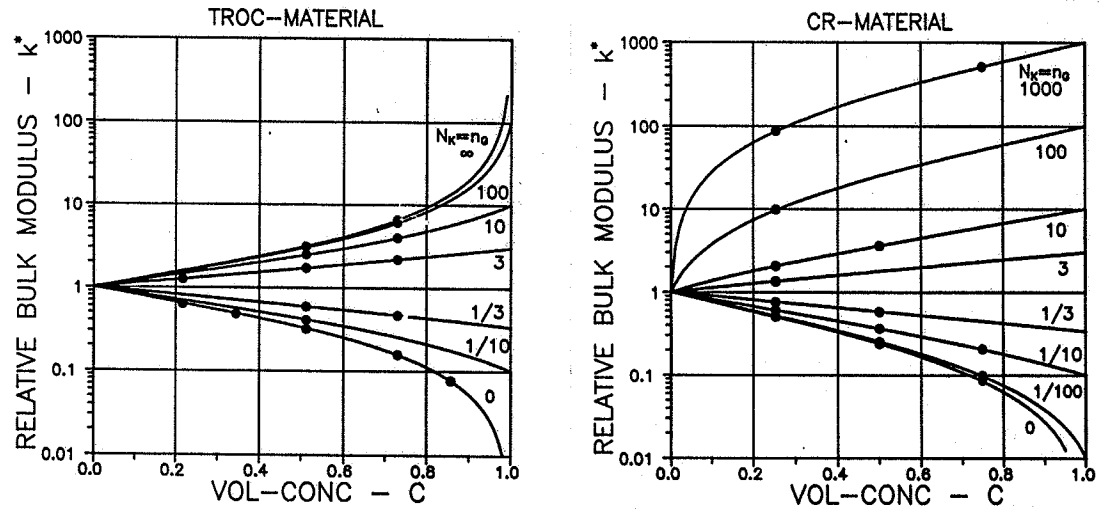

Figure 3. Bulk moduli of TROC- and CR-materials. Dots: FEM-analysis (10,11). Lines: Theoretically predicted moduli.

III. STRESS AND STRAIN IN COMPOSITE MATERIAL

In this section we consider stress and strain in a composite subjected to hygro-thermal action. The constituent phases are at first solid. Realizing, however, that many real composites like impregnated materials can not be modelled in this way modifications are introduced in a separate sub-section which consider the situation of one phase being porous.

Mechanical load: The following expressions considering average stress and average strain in a composite loaded by σ_{kk} are obtained from (1). They are exact which can easily be checked by the work of Hill (12).

$$\sigma_{S,kk} = \frac{1/n_K - 1/k^*}{(1-c)(1/n_K - 1)} \sigma_{kk} \quad ; \quad \sigma_{P,kk} = \frac{1/k^* - 1}{c(1/n_K - 1)} \sigma_{kk} \qquad (13)$$

$$\epsilon_{S,kk} = \frac{k^* - n_K}{(1 - c)(1 - n_K)} \, \epsilon_{kk} \quad ; \quad \epsilon_{P,kk} = \frac{1 - k^*}{c(1 - n_K)} \, \epsilon_{kk} \qquad (14)$$

Hygro-thermal load: We now consider a composite material exposed to hygro-thermal action. The *composites free hygro-thermal strain, α_{kk},* is defined by the volume strain which is hereby experienced by the composite. The free (unrestraint) hygro-thermal strains of phase S and P are $\alpha_{S,kk}$ and $\alpha_{P,kk}$ respectively.

α_{kk} and the phase stresses $\sigma_{S,kk}$ and $\sigma_{P,kk}$ set up by the hygro-thermal strain differences can be determined as follows by Equations 13 and 14 (with $\epsilon_{kk} = \alpha_{kk}$) utilizing additionally that the volumetric stress average must be 0 (no external load),

$$c\sigma_{P,kk} + (1 - c)\sigma_{S,kk} = 0 \qquad (15)$$

The composite is loaded fictitiously with $\sigma^P{}_{kk}$ such that a) phase P obtains its free hygro-thermal strain, which at the same time b) will make phase P stress free.

$$a) \quad \alpha_{kk} + \frac{\sigma^P_{kk}}{3K^*} = \alpha_{P,kk} \qquad (16)$$

$$b) \quad \sigma_{P,kk} + \sigma^P_{kk} \, \frac{1/k^* - 1}{c(1/n_K - 1)} = 0 \qquad (17)$$

The fictitious load, $\sigma^P{}_{,kk}$, can be eliminated from these equations producing the following relation between free composite hygro-thermal strain, α_{kk}, and phase P stress, $\sigma_{P,kk}$,

$$\alpha_{kk} = \alpha_{P,kk} + \frac{\sigma_{P,kk}}{3K^*} \, \frac{c(1/n_K - 1)}{1/k^* - 1} \qquad (18)$$

A relation between free composite hygro-thermal strain, α_{kk}, and phase S stress, $\sigma_{S,kk}$, is obtained in a similar way – now applying a fictitious load, $\sigma^S{}_{kk}$, to obtain a stress free phase S. We get

$$a) \quad \alpha_{kk} + \frac{\sigma^S_{kk}}{3K^*} = \alpha_{S,kk} \qquad (19)$$

$$b) \quad \sigma_{S,kk} + \sigma^S_{kk} \, \frac{1/n_K - 1/k^*}{(1 - c)(1/n_K - 1)} = 0 \qquad (20)$$

by which the following relation is produced between free composite hygro-thermal strain, α_{kk}, and phase S stress, $\sigma_{S,kk}$,

$$\alpha_{kk} = \alpha_{S,kk} + \frac{\sigma_{S,kk}}{3K^*} \, \frac{(1 - c)(1/n_K - 1)}{1/n_K - 1/k^*} \qquad (21)$$

The free composite hygro-thermal strain and the internal stresses are now obtained combining Equations 15, 18 and 21 and introducing the hygro-thermal strain difference, $\Pi_{kk} = \alpha_{P,kk} - \alpha_{S,kk}$. We get

$$\alpha_{kk} = \alpha_{S,kk} + \Pi_{kk} \, \frac{1/k^* - 1}{1/n_K - 1} \quad ; \quad \Pi_{kk} = \alpha_{P,kk} - \alpha_{S,kk} \qquad (22)$$

$$\sigma_{P,kk} = 3K^*\eta_{kk} \frac{(1/k^* - 1)(1/k^* - 1/n_K)}{c(1/n_K - 1)^2} \qquad (23)$$

$$\sigma_{S,kk} = -3K^*\eta_{kk} \frac{(1/k^* - 1)(1/k^* - 1/n_K)}{(1 - c)(1/n_K - 1)^2} \qquad (24)$$

The problem of hygro-thermal loading of composites has also been considered by other authors. Quantitatively Equation 22 is identical to a more complex expression given in (13) on the coefficient of thermal expansion of composites. The shrinkage problem in concrete has been studied in (e.g. 14,15,16,17). Thermal expansion of particle-reinforced materials in general has been studied in (e.g. 18,19). A general review on the physical properties of composite materials is given in (20). The present study of the problem has the advantage of reflecting the influence of any phase geometry and at the same time predict the internal composite stresses.

Equations 22 - 24 relate internal stresses as follows to difference between free volume strains of composite and phase S,

$$c\sigma_{P,kk} = -(1-c)\sigma_{S,kk} = 3K^*(\alpha_{kk} - \alpha_{S,kk}) \frac{1/k^* - 1/n_K}{1/n_K - 1} \qquad (25)$$

When *porous materials* especially are considered with $n_K = 0$ Equation 25 reduces as follows relating volume expansion of porous material to *pore pressure*

$$\alpha_{kk} - \alpha_{S,kk} = -c \frac{\sigma_{P,kk}}{3K^*} = (1-c) \frac{\sigma_{S,kk}}{3K^*} \qquad (26)$$

Shrinkage of a composite material with only phase S shrinking is immediately given by Equation 22. We get

$$\frac{\alpha_{kk}}{\alpha_{S,kk}} = \frac{1/n_K - 1/k^*}{1/n_K - 1} = \begin{cases} 1 & \text{when } n_K = 0 \\ 1 - c & \text{when } n_K = 1 \\ 1/k^*_\infty & \text{when } n_K = \infty \end{cases} \qquad (27)$$

Impregnated materials

Lamella composites include porous materials where pores (phase P) have been impregnated by solidification of a liquid. For several reasons such a procedure may cause incomplete impregnation leaving empty pore space. A stress-strain analysis of impregnated porous materials exposed to hygro-thermal action can be made as explained in the preceding sections for lamella composites introducing the effective phase P stiffness and hygro-thermal properties suggested in the following text. The question of stress-strain caused by volume change of liquid due to solidification is also considered here. A free effective solidification pore phase strain, $\Gamma_{P,kk}$, is suggested by which the problem of impregnant solidification can be solved like the problem of hygro-thermal action previously considered simply by replacing $\alpha_{P,kk}$ with $\Gamma_{P,kk}$. The terminology applied is explained in the following list.

β *Pore saturation of solidifiable liquid. (Volume impregnant relative to pore volume).*

$\alpha_{PS,kk}$ *Free volumetric hygro-thermal strain of solid impregnant*
$\Gamma_{PS,kk}$ *Free volumetric solidification strain of impregnant*
$\Gamma_{P,kk}$ *Free volumetric solidification strain of pore phase*
Γ_{kk} *Free volumetric solidification strain of composite*
K_{PS} *Bulk modulus of solid impregnant.*
E_{PS} *Young's modulus of solid impregnant.*
v_{PS} *Poisson's ratio of solid impregnant.*

The pore saturation may depend on temperature and pore size. Water in very narrow pores, for example, may still not be frozen at a temperature of - 10 °C. Pore saturation β "counts" only the freezable part of the water.

Effective pore phase stiffness: The effective phase P bulk modulus is estimated considering phase P to be a porous material where pores are volume not occupied by the impregnant. We introduce the following "pore" parameters, $(c, c_d, \mu_o, M) = (1-\beta, 1, A, 0)$, and get by Equations 7 and 8 (with $\Theta_S \approx 1$)

$$K_P = K_{PS} \frac{A\beta}{1 + A - \beta} \tag{28}$$

where flat voids and spherical voids have $A \approx 0.3$ and $A \approx 1$ respectively. The effective Young's modulus of the pore system can be approximated to vary with saturation in the same way as K_P, meaning $E_P/E_{PS} \approx K_P/K_{PS}$. The effective Poisson's ratio can then be considered a constant, meaning $v_P \approx v_{PS}$. It is noted that we have implicitly assumed that stiffness moduli developed by solidification of liquid is independent of restraint (pressure or tension).

Effective free hygro-thermal strain of pore phase: Hygro-thermal strain of a porous material is known (e.g. 17,21) to be invariant with respect to porosity. Thus

$$\alpha_{P,kk} = \alpha_{PS,kk} \tag{29}$$

Effective free solidification strain of pore phase: Looking at the pore phase as an ideal smooth and continuous system no gross (visible) volume expansion and pore pressure will be observed at solidification of impregnant before $\beta > 1/(1+\Gamma_{PS,kk})$. Real pore walls, however, are not smooth and many narrow necks will provide conditions obstructing the free flow of impregnant, such that the "build in" solidified impregnant also at $\beta < 1/(1+\Gamma_{PS,kk})$ will produce pore pressure (or tension) corresponding to an effective free solidification strain, $\Gamma_{P,kk}$.

Generally it is impossible to quantify this statement theoretically. The problem to solve is too complex involving pore size distribution and a number of un-known quantities like type of pore wall texture for example. At the present we have no other choice than proceed suggesting a plausible expression relating $\Gamma_{P,kk}$ to pore saturation such that $\Gamma_{P,kk} = 0$ and $\Gamma_{P,kk} = \Gamma_{PS,kk}$ are predicted at $\beta = 0$ and 1 respectively. We suggest the following simple type of expression which produces the "steeper" variation between $\beta = 1/(1+\Gamma_{PS,kk})$ and $\beta = 1$,

$$\Gamma_{P,kk} \approx \beta\Gamma_{PS,kk}[B + (1-B)\beta^{1/[(1-B)!\Gamma_{PS,kk}!]}] \qquad (30)$$

where the *efficiency factor* B < 1 has to be determined experimentally. The factor will increase with increasing "roughness" of pore walls and amount of narrow pores.

IV. PREDICTION METHOD

The information obtained in Section II and III are now integrated to form a method of predicting the effects of hygro-thermal and similar actions on isotropic two-phase materials of arbitrary internal geometry. In general no part of the method can be solved analytically. The method is therefore presented as an algorithm where input data and steps of calculations are arranged for computer examination of the problem. The symbol < > indicates effective quantities of phase P (considering solidification strain and incomplete impregnation) such that calculation can proceed considering phase P to be "solid". We superimpose solidification strain and hygro-thermal strain assuming here that the latter strain is given *"per unit moisture content or temperature"*, T.

To *support* an estimate of the shape factor, $\mu'_o \leq 1$, we may use the following expression which considers phase geometry to be pseudo-symmetric.

$$\mu'_o = \mu_o\left(\frac{1 - c_D}{c_d}\right)^M \qquad (31)$$

Input: Materials properties

Stiffness:	$E_P(E_{PS})$, $v_P(v_{PS})$, E_S, v_S
Geometry:	c_d, c_D, μ_o, μ'_o, $M(=1)$
Voids in impregn.	A ($\approx 1/3$)
Vol.hygro-therm.strain/T:	$\alpha_{P,kk}(\alpha_{PS,kk})$, $\alpha_{S,kk}$
Increase in T (moist.temp.)	$\cap T$
Free vol.solidific. strain:	$\Gamma_{PS,kk}$
Efficiency factor:	B (≈ 0.02)

Independent variables

Volume concentration: c
Pore saturation: β

Auxiliary quantities

$$\langle n \rangle = \frac{E_{PS}}{E_S} \frac{A\beta}{1 + A - \beta} \quad ; \quad \langle n_K \rangle = \langle n \rangle \frac{1 - 2v_S}{1 - 2v_{PS}}$$

$$\langle n_G \rangle = \langle n \rangle \frac{1 + v_S}{1 + v_{PS}} \quad ; \quad \Theta_S = 2\frac{1 - 2v_S}{1 + v_S}$$

$$\langle \alpha_{P,kk} \rangle = \alpha_{PS,kk}\cap T + \beta\Gamma_{PS,kk}[B + (1-B)\beta^{1/[(1-B)!\Gamma_{PS,kk}!]}]$$

Composite stiffness

Shape functions: Equation 10
Geometry function: Equation 4
Relative bulk modulus: Equation 3

Composite stress and strain

Phase P stress: Equation 23
Phase S stress: Equation 24
Composite strain: Equation 22

Output

Listings of composites strain, stress and bulk modulus as functions of porosity c, or pore saturation β, of impregnant

V. APPLICATIONS

The power of the prediction method developed is demonstrated in this section on 1) Shrinkage of particulate material and lamella material, 2) Thermal expansion of salt impregnated bricks, 3a) Internal stresses build up by freezing of water in bricks, and 3b) Frost resistance of wet bricks. Theoretical results are evaluated by the algorithm presented in Section IV.

Example 1 - Shrinkage

The TROC-material and CR-material previously referred to are considered with a shrinking phase S. The elastic moduli are $E_P = 5E_S$ and $v_P = v_S = 0.2$. The predicted composites shrinkage and internal stresses are shown in Figure 4. It is noticed that a lamella phase P reduces shrinkage much more than a particle phase P. This feature becomes extremely significant when $n_K \rightarrow \infty$.
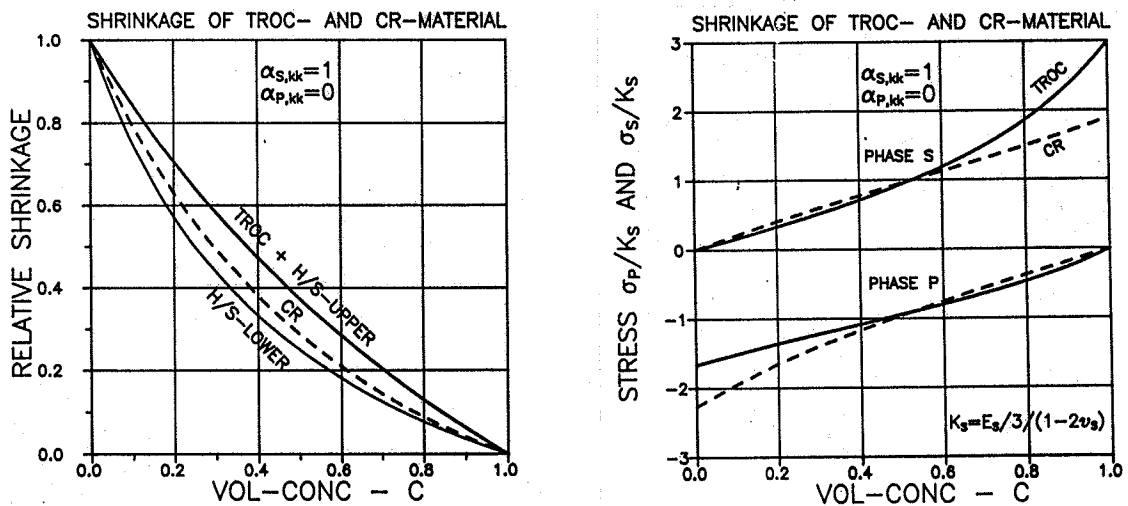

Figure 4. TROC-material and CR-material. ■ Shrinkage. ■ Internal stresses. Theoretically predicted quantities. Example 1.

Comments: Portland cement concrete can in many ways be considered as a particle reinforced material. Phase S is cement paste which shrinks and phase P is aggregate (sand and gravel) which does not shrink. A commonly used rule (e.g.22) is that relative shrinkage of

concrete is proportional to $\approx (1 - c)^{1.4}$ which is of the same order of magnitude applying to TROC shrinkage in Figure 4.

Example 2 - Thermal expansion

The thermal expansion of salt infected (impregnated) bricks has been determined experimentally in (23) as related to porosity and weight amount of salt (NaCl). The results are shown by dots in Figure 5. Thermal expansion coefficients of plain rock salt (phase P) and plain tile salt (phase S) were determined to be $\alpha_P = 38*10^{-6}/^oC$ and $\alpha_S = 6*10^{-6}/^oC$ respectively. The Young's moduli were $E_P = 15000$ MPa and $E_S = 14000$ MPa. Both Poisson's ratios are approximately 0.2. A mean pore saturation of salt of $\beta = 0.20$ can be deduced from the experimental data. All saturation data (except one, obviously false) were bounded by $0.15 < \beta < 0.25$.

The lines shown in Figure 5 represent expansion and phase stresses theoretically predicted with $(c_d,c_D,\mu_o,\mu'_o,M) = (0.6,0.0,0.75,1.0,1)$ describing a materials model where a continuous matrix is penetrated by continuous pores $(c_D = 0)$ which dissolve the matrix phase into particles at $c = c_d = 0.6$. The pores have pockets at low concentrations $(\mu_o = 0.75)$. The (fictitious) matrix phase particles at $c \approx 1$ are spherical $(\mu'_o = 1)$. A shape factor of $A = 0.35$ is assumed for voids in impregnant (salt). Also shown in Figure 5 are the upper and lower bounds on expansion which are obtained introducing composite stiffness as given by the H/S-bounds previously referred to.
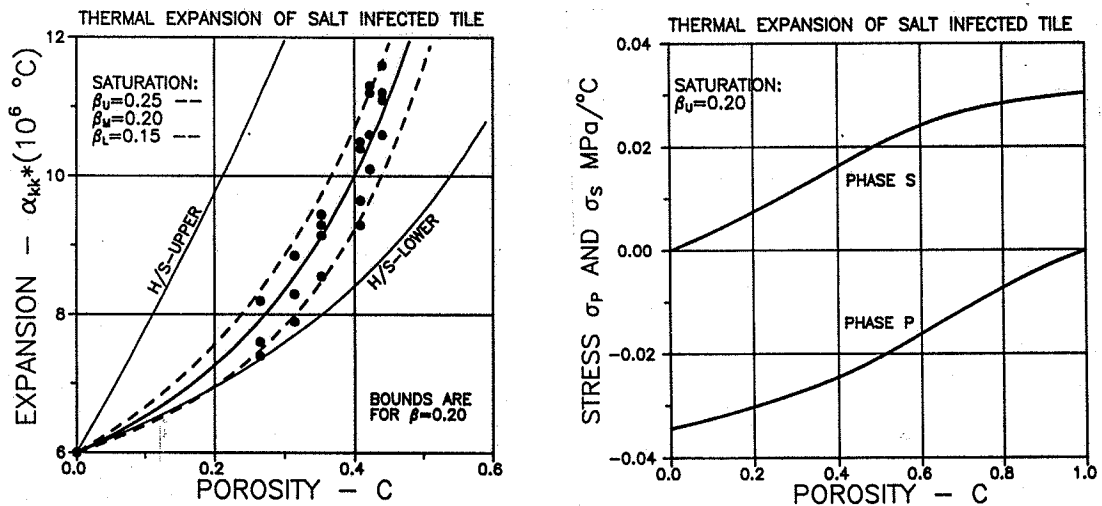

Figure 5. Salt infected tile. ▪ Thermal expansion. ▪ Internal stresses. Dots: Experimental expansion data from (23). Lines: Theoretically predicted quantities. Example 2.

Example 3 - Frost

We now look at bricks with the same geometrical and elastic properties as those considered in Example 2. The empty pores are impregnated with water which is then solidified to ice lowering the temper-

ature. Given the following additional data (24,25). ■ *Ice:* E_P = 9000 MPa, v_P ≈ 0.2. Volumetric solidification of water -> ice, $\Gamma_{PS,kk}$ = 0.09. ■ *Tile:* High temperature fired: Porosity, c ≈ 0.3, Tensile strength, S = 6 - 10 MPa. Normal temperature fired: (c,S) ≈ (0.4, 4-8 MPa). Low temperature fired: (c,S) ≈ (0.5, 2-6 MPa). ■ As a first approximation we neglect thermal expansion ($\alpha_{P,kk}$ = $\alpha_{S,kk}$ = 0) and consider only water which is freezable. An efficiency factor of B = 0.02 is assumed in Equation 30 when pore pressures are considered at saturations, β < 1.
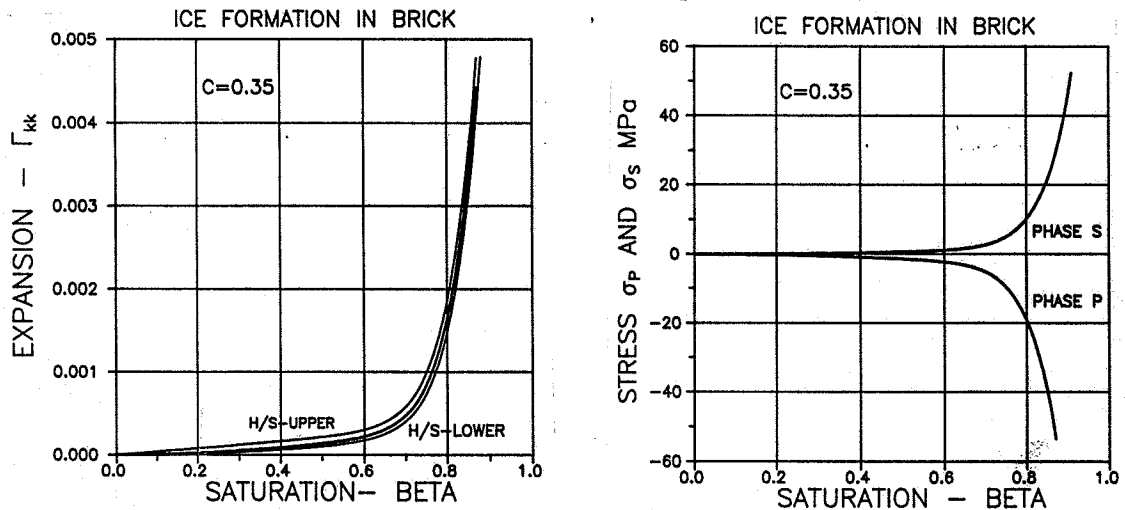

Figure 6.   Frost in water impregnated brick. ■   Expansion due to ice formation. ■   Stresses set up by ice formation. Theoretically predicted quantities. Example 3a.

Problem a: Ice is formed in a brick of porosity 35 %. Predict brick expansion and internal stresses as a function of pore saturation. ■ The predicted results are presented graphically in Figure 6. It is noticed that both brick expansion and solid phase tensile stress increase steeply at β > 0.7. The latter feature may cause brick failure as the solid structures strength is approached. This phenomenon is considered in the following problem.

Problem b: Brick damage may appear at a certain *critical pore saturation*, β_{CR}. Predict β_{CR} as a function of porosity and tensile strength of the three brick types previously described. ■ The predicted results are shown in Figure 7. They are obtained introducing a maximum $\sigma_{S,kk}$ = $3S_P$ where S_P is "pore strength" given by the following expression derived in Appendix B,

$$S_P \approx \frac{S}{(1 - \mu_o^2)^{1/2}} \qquad (32)$$

It is emphasized that the Example 3 analysis is based on an estimate, B = 0.02, of the efficiency factor appearing in Equation 30. The estimate, however, might be quite reasonable. Critical pore saturations of β_{CR} ≈ 0.75 for bricks were observed experimentally by Fagerlund

(26) who has published a number of papers (e.g. 27,28) on freezing of porous materials.

Comments on frost resistance: We recall that β is relative amount of freezable water. For most real porous materials this means that β = 100 % is a highly theoretical quantity which can only be approached at high pressure impregnation and extremely low temperatures where ice formation can occur also in narrow pores. In practice pore saturation is very much dependent on *environment and pore size distribution.* Examples on water uptake mechanisms are: ■ A) sorption (from damp atmosphere), ■ B) suction (from damp atmosphere and contact with water surface), and ■ C) water submergence. The amount of water uptake increases in the order A - C, meaning that large pores have low A and B pore saturations. Thus, if the amount of large pores is relatively high, then the porous material considered may always be frost resistant under conditions A and B, while the material may be frost damaged under condition C.

FROST DAMAGE CRITERION FOR BRICKS
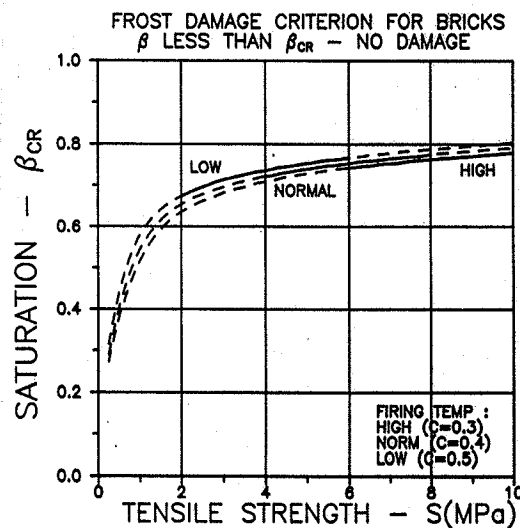β LESS THAN β_{CR} — NO DAMAGE

Figure 7. Critical pore saturation of water in bricks below which no frost damage will appear. Theoretically predicted quantities. Example 3b.

It is noticed from Figure 6 that the phase S tension increases steeply in the area β ≈ 0.7 - 1. This means that even a slight decrease in pore saturation at A and B water uptakes may increase considerably the frost resistance of the porous material considered. Adding a relatively small amount of relatively large spherical air bubbles to concrete, for example, does improve frost durability (e.g.29). An additional positive effect in this respect is that air bubbles act as crack arresters and increase the effective shape factor, μ_o, which increase pore strength, see Equation 32.

VI. FINAL REMARKS

A rational method has been developed which predicts stress and strain in two-phase materials exposed to hygro-thermal action or sim-

ilar actions like volume change by solidification or freezing of liquid impregnant in porous materials.

The most important feature of the method is its ability to consider arbitrary phase geometries - from perfectly particle reinforced materials to perfectly laminated materials. This means, for example, that the method can be used in *materials design* - or in *detection of materials destruction* by comparing physical properties as determined by theory and by experiments respectively. Destruction changes the internal geometry of composites which is reflected by spontaneous deviation from theoretically expected materials behavior. A recent work by the present author (3) might be of interest in this respect where stiffness-strength relations are developed for porous materials. Other physical properties like thermal and electric conductivity, dielectric constants and magnetic permeability for example may also be thought of in the context of damage detection in composites. Basic information on this subject is presented in Appendix A.

Optimal behavior prediction of composites and optimal design of such materials depend very much on knowledge on the influence of phase geometries. A number of high priority future research projects are hereby defined including consistent quantifications by shape functions of phase geometry distributions. Thorough studies on pore size distributions in clay bricks (30), for example, is the first step to establish a safe frost damage criterion for this material or to improve its stiffness and strength qualities by pore modification. Studies are presently made by the author (31,32) involving residual physical properties of frost damaged porous materials as related to pore characteristics. A subsequent paper deals with this and related problems like strength reduction by alkali-aggregate reactions (e.g. 33) in cementitious materials. Parallel experimental studies are made by the author and the concrete division of AE-Consult, Denmark.

Finally: ▪ It is noticed that the influence of hygro-thermal and similar actions on plane isotropic two phase composites (like wood) can be analyzed in exactly the same way as given in this paper for isotropic composites. The basic information needed for this purpose are available in (1). ▪ A number of building materials behave viscoelastically. Procedures are demonstrated in (e.g. 2,17,21,34) by which the results obtained in the present analysis can be generalized also to apply when linear-viscoelastic composites are considered. ▪ The expressions given in Section II to predict bulk modulus of a composite material apply in principle also when shear modulus and Young's modulus are considered. Only a few simple modifications explained in (1) have to be introduced. Good estimates, however, can be obtained directly when Poisson's ratios are approximately 0.2.

APPENDIX A

Other physical properties

It is well-known (e.g. 20) that a number of physical properties of composites (*like thermal and electric conductivity, dielectric constant and magnetic permeability*) are related to the properties of the constituent phases in a way which is analogous to the relations considering stiffness properties. Bounds on the dielectric constants of isotropic two phase composites were developed by Hashin and Shtrik-

man in (35). It is shown in (1) that any of the physical properties just referred to are described by the present stiffness theory only by introducing $v_S = v_P = 0 \Rightarrow \theta_S = 2$. Thus, when Q is the physical property considered we get by Equations 3 and 4

$$q^* = \frac{Q^*}{Q_S} = \frac{n + \langle\theta\rangle[1 + c(n - 1)]}{n + \langle\theta\rangle - c(n - 1)} \quad ;(n = Q_P/Q_S) \quad (A1)$$

where the influence of phase geometry is introduced by the following geometry function, $2 \leq \langle\theta\rangle \leq 2n$,

$$\langle\theta\rangle = \mu + n\mu' + \sqrt{(\mu + n\mu')^2 + 4n(1 - \mu - \mu')} \quad (A2)$$

and shape functions μ and μ' are the same (Eq. 10) as used in the main text predicting bulk modulus.

The following rough estimate on a relation between critical concentration, c_d, and shape factor, μ_o, is obtained comparing the results obtained by the present theory with the dilute spherical dispersion mixture relation developed by Rayleigh (36) and the dielectric constant solution obtained by the Böttcher SCS-approximation (37) (Self Consistence Scheme) for spheres of finite concentration in a continuous matrix.

$$c_d \geq \frac{2\mu_o}{1 + 2\mu_o} \quad (A3)$$

APPENDIX B

Pore strength

Pore strength is the particular (hydraulic) pore pressure which just causes cracks to become unstable. Pore strength, S_P, is related approximately to uni-axial strength, S, by the following arguments advanced by the author in (31,32):

Strength of porous materials externally loaded have been considered successfully in (3) with pores modelled by "pore cracks" (circular tunnels or spheres of diameters 2L with crossing concentric cracks of diameter 2l (> 2.5L)). We now replace external load with a (hydraulic) pore pressure, σ_P (also acting in crack zones) and consider the appropriate stress intensity factor given in (38) applying for a hole of diameter 2L crossed by a co-centered crack of length 2l (> 2L),

$$K = \sigma_P\sqrt{\pi l} * f(L/l) \quad ; \quad f = f(L/l) \quad (B1)$$

The correction factor given in (38) can be related approximately to shape factor, μ_o, as follows introducing the logarithmic mean, $\mu_o \approx (L/l)^{2\cdot5}$, of the orders of magnitudes, $\mu_o \approx (L/l)^2$ and $\mu_o \approx (L/l)^3$ applying for tunnel pore cracks and spherical pore cracks respectively (3). We get

$$f \approx (1 - \mu_o^2)^{1/2} \quad (B2)$$

Now, comparing the pore pressure stress intensity factor in Equation B2 with the basic factor used in (3), namely $K = \sigma\sqrt{(\pi l)}$ applying for uni-axial tension, σ, it is obvious that pore strength and conventional

tensile strength are related as given in Equation 32 in the main text of the paper.

References

1) Nielsen, L. Fuglsang: "Elastic Properties of Two-Phase Materials". *Mater. Sci. Eng.*, 52(1982), 39 - 62.

2) Nielsen, L. Fuglsang: "Elasticity and Damping of Porous Materials and Impregnated Materials". *Journ. Am. Ceramic Soc.*, 67(1984), 93 - 98.

3) Nielsen, L. Fuglsang: "Strength and Stiffness of Porous Materials". *Journ. Am. Ceramic Soc.*, 73(1990), 2684 - 89.

4) Nielsen, L. Fuglsang: *"Strength of hardened cement paste - On the relevance of Bolomey and Ryshkewitch descriptions"*. Tech. Univ. Denmark, Build. Mat. Lab., tech report tr-211(1990).

5) Hashin, Z. and Shtrikman, S.: "Variational approach to the theory of elastic behavior of multi-phase materials". *J. Mech. Solids*, 11(1963), 127 - 140.

6) Hashin, Z.: *J. Appl. Mech.*, 29(1962), 143

7) Budiansky, B.: On the elastic moduli of some heterogeneous materials". *J. Mech. Phys. Solids*, 13(1965), 223 - 227.

8) Paul, B.: "Prediction of elastic constants of multi-phase materials". *Trans. of the Metallurgical Soc. of AIME*, 218(1960), 36 - 41.

9) Hansen, T.C.: "Creep of concrete: A discussion of some fundamental problems". *Bulletin no. 33(1958)*, Svenska Forskningsinstitutet för Cement och Betong, Tekniska Högskolan, Stockholm".

10) Nielsen, L. Fuglsang: *"Elastic Properties of isotropic particle reinforced materials and phase-symmetric materials"*. Tech. Univ. Denmark, Build. Mat. Lab., Tech. Report 54(1977).

11) Nielsen, L. Fuglsang: *"Elastic Properties of two-phase Materials"*. Tech. Univ. Denmark, Build. Mat. Lab., Tech. Report 82(1980).

12) Hill, R.: "Elastic properties of reinforced solids: Some theoretical principles". J. Mech. Phys. Solids, 11(1963), 357 - 372.

13) Levin, L.M.: *Mekhanika Tverdogo Tela*, 1(1967), 88.

14) Pickett, G.: "Effect of aggregate on shrinkage of concrete", *Journ. Am. Concrete Inst.* 52(1956), 581.

15) Hansen, T.C. and Nielsen, K.E.C.: "Effect of aggregate properties on concrete shrinkage". *Journ. Am. Concrete Inst.*, 62(1965), 783.

16) Nielsen, K.E.C.: *"Aggregate stresses in concrete"*. Thesis, Proc. 41(1971), Swedish Cement and Concrete Res. Inst., Techn. Univ. of Stockholm, Sweden.

17) Nielsen, L. Fuglsang: "Interne Spannungen sowie Schwind- und Temperaturdeformationen des Betons", *Cem. Concr. Res.*, 4(1974), 31 - 44.

18) Sendeckyi, G.P.: "Elastic Behavior of Composites", pp 46 - 83 in *Composite Materials: Vol. II: Mechanics of Composite Materials"* (ed. Sendeckyi, G.P.), Academic Press, New York 1974.

19) Chow, T.S.: "The effect of particle shape on the mechanical properties of filled polymers". *Journ. Materials Science*, 15(1980), 1873-88.

20) Hale, D.K.: "The physical properties of composite materials". *Journ. Materials Science*, 11(1976), 2105-41.

21) Nielsen, L. Fuglsang: "Rheologische Eigenschaften für isotrope linear-viskoelastische Kompositmaterialien". Cement and Concrete res., 3(1973), 751 - 766.

22) Markestad, A. and Maage, M.: *"Building Materials, Vol II"*, (norwegian), textbook, TAPIR, Trondheim, Norway, 1978.

23)   Larsen, E.S. and Nielsen, C.B.: "Decay of bricks due to salt". *Materials and Structures*, 23(1990), 16 - 25.

24)   Hansen, E. dePlace: *"Frost resistance and strength of tile"* (in danish) and ∎ Schmidt, L. and dePlace Hansen, E.: "*Frost resistance of tile"* (in danish). Tech. Univ. Denmark, Build. Mat. Lab., Tech. reports 210(1990) and 203(1989) respectively.

25)   Nielsen, A.: *"Materials Data"*. In "Building Materials" (textbook in danish), 25 - 36. Tech. Univ. Denmark, Build. Mat. Lab., 1986.

26)   Fagerlund, G.: *"Critical water saturation related to freezing of porous and brittle materials"* (in swedish). Inst. Build Tech., Tech. Univ. of Lund, Sweden, Tech. report 34(1972)

27)   Fagerlund, G.: *"Significance of critical degrees of saturation at freezing of porous and brittle materials"*. Inst. Build Tech., Tech. Univ. of Lund, Sweden, Tech. report 40(1973).

28)   Fagerlund, G.: "Principles of frost durability of concrete" (in swedish). *Nordisk Betong*, 2(1981).

29)   Powers, T.C.: "The air requirement of frost-resistant concrete". Highway Res. Board, (Washington, D.C.), Proc. 29(1949), Research and Develop. Labs. Portland Cement Assoc. Res Dept. Bull. 33.

30)   Hansen, W. and Kung, J.H.:: "Pore structure and frost durability of clay bricks". *Materials and Structures*, 21(1988), 443 - 447.

31)   Nielsen, L. Fuglsang: *"Self-destruction of impregnated porous materials"* (in danish). Tech. Univ. Denmark, Build. Mat. Lab., tech report tr-192(1988).

32)   Nielsen, L. Fuglsang: *"Frost damage in porous materials - a prediction procedure"* (in danish). Tech. Univ. Denmark, Build. Mat. Lab., tech report tr-197(1989).

33)   Bredsdorff, P., Idorn, G.M., Kjær, A., Plum, N.M., and Poulsen, E.: "Chemical reactions involving aggregate". In "Chemistry of Cement", U.S. Department of Commerce, National Bureau of Standards Monograph, 43(1962), Vol II, 749 - 806 (incl. discussions).

34)   Nielsen, L. Fuglsang: *"Materials Mechanics"* (in danish). Textbook, Build. Mat. Lab., Tech. University of Denmark. Tech. Report 189(1988).

35)   Hashin, Z. and Shtrikman, S., *J. Appl. Phys.*, 33(1962), 3125.

36)   Rayleigh, J.W., *Phil. Mag.*, 34(1892), 481.

37)   Böttcher, C.J.F., *Rec. Trav. Chim. Pays-Bas*, 64(1945), 47.

38)   Murakami (Ed.), *"Stress intensity factors handbook"*, Vols. I and II. Pergamon Press, New York, 1987.